Research Article

Prediction of Mechanical Strength by Using an Artificial Neural Network and Random Forest Algorithm

Kamal Upreti [ID],[1] Manvendra Verma,[2] Meena Agrawal,[3] Jatinder Garg,[4] Rekha Kaushik,[5] Chinmay Agrawal,[6] Divakar Singh,[7] and Rajamani Narayanasamy [ID][8]

[1]*Department of Computer Science & Engineering, Dr. Akhilesh Das Gupta Institute of Technology and Management, New Delhi, India*
[2]*Department of Civil Engineering, Dr. Akhilesh Das Gupta Institute of Technology and Management, New Delhi, India*
[3]*Energy Center, Maulana Azad National Institute of Technology, Bhopal, India*
[4]*Department of Mechanical Engineering, Baba Hira Singh Bhattal Institute of Engineering & Technology, Lehragaga, Punjab, India*
[5]*Department of Electronic & Comm. Engineering, Maulana Azad National Institute of Technology, Bhopal, India*
[6]*Department of Civil Engineering, Indian Institute of Technology, Ropar, Punjab, India*
[7]*Department of Computer Science & Engineering, UIT, Barkatullah University, Bhopal, Madhya Pradesh, India*
[8]*Department of Mechanical and Energy Engineering, College of Science and Technology, University of Rwanda, Rwanda*

Correspondence should be addressed to Rajamani Narayanasamy; n.rajamani@ur.ac.rw

Geopolymer concrete could be the best alternative to ordinary Portland cement concrete due to its higher performance in any severe condition. It reduces the carbon footprints to a very higher level. Machine learning methods are the future of the construction industry because it predicts the mechanical strengths of concrete mix design on the basis of their constituents without destructive test conduction. This study is aimed at developing the models to predict the mechanical strengths and validate them with the actual results. After the experimental investigation, we found the results of the mechanical (including compressive, splitting tensile, and flexural tensile) strength. The M2 mix of geopolymer concrete got the highest mechanical strengths whereas the M5 mix gets the lowest mechanical strengths among all the mix designs. The machine learning methods ANN (artificial neural network) and random forest are used to develop the models based on mixed experimental results. Mechanical strength results are taken as outputs, and mixed constituents are taken as inputs for training and testing. The performance of predicted results is checked based on R^2, MAE (mean absolute error), RMSE (relative mean square error), RAE (relative absolute error), and RRSE (root-relative square error). Random forest models show the best prediction to the ANN models because it shows the negligible error between actual and predicted values. The R^2 value is 1 of 12 predicted results out of 15 by the use of random forest methods. So it is most suitable to predict the strength of geopolymer concrete based on their constituent's material quantity.

1. Introduction

Concrete is a very important material for our society and nation because the development of infrastructures is built primarily on concrete [1]. Concrete is the second most used material in the world after the water [2]. The production of concrete increases exponentially day by day [3, 4]. Portland cement is an essential and primary material for the production of ordinary concrete [5]. Around one ton of carbon dioxide is produced during the production of one-ton cement. The higher carbon dioxide emissions cause global warming [6, 7]. It deteriorates the ice of the Arctic and Antarctica mountains near the north and south poles of the earth [8]. Carbon dioxide shares around 50% of emissions among all greenhouse gases [9]. The cement industries contribute to around 8 percent of carbon dioxide emissions. So the production of concrete directly contributes to the increment in global warming.

Geopolymer is highly effective over conventional concrete due to better strength, durability, and performance in various severe conditions also [10–12]. It shows better resistance to acid attack, sulphate attack, elevated temperatures, and freeze-thaw, wetting-drying, and seawater conditions [13–15]. It is eco-friendly, economic, and sustainable concrete over conventional concrete. It directly affects the circular economy through the usage of industrial symbiosis. The various factors that affect the properties of the geopolymer concrete would be curing condition and temperature, the molarity of sodium hydroxide, alkaline ratio, superplasticiser dosage and type, liquid to binder ratio, fly ash and GGBFS contents and composition, and gradation of aggregates [14–22].

The above-defined problem could be reduced by the production of geopolymer concrete, because it would replace the cement content with pozzolanic materials like fly ash, GGBFS, rice husk ash, and calcined clay (metakaolin) [23–26]. The production of geopolymer concrete directly reduces the emission of carbon dioxides around 80 percent of ordinary concrete production [27]. The geopolymer is a name of bonding that is firstly stated by Prof. Davidovits in 1978. The geopolymer concrete is made with a different bonding pattern than the Portland cement bonding, in which the alkaline solution is used to activate the pozzolanic material to react with each other. Sodium or potassium hydroxide and sodium or potassium silicate are used as alkaline solutions in the geopolymer concrete [28–34]. It reacts with the alumino-silicates that are present in the pozzolanic material and make bonds. It makes the bond-like K^+ or Na^+-$(Al-O-Si-O)_n - xH_2O$, whereas the calcium silicate hydroxide (C-S-H) bonds are made in the Portland cement reaction. Geopolymerisation is a process of reaction to build geopolymer bonds from the basic constituents. It occurs during the reaction of alumino-silicate to alkaline solution in the presence of water to make up to end products [35]. The geopolymer concrete is highly resistant to acid attack, sulphate attack, seawater conditions, freeze-thaw conditions, and other severe conditions compared to ordinary Portland cement concrete [36, 37]. The geopolymer concrete is easily usable in the construction of columns, beams, piles, and slabs. It can also be usable in the stabilization of soils by the mixing of materials with the weaker soils [38]. The geopolymer constituents are fly ash, GGBFS, sodium hydroxide, sodium silicate, superplasticiser, aggregates, and water. The mechanical property analysis is done over many years, in which various research stated the optimum point to get maximum strength and performance.

The alkali-activated concrete and geopolymer concrete are different due to their reaction occurring during strength and hardenings. In both concrete, the constituents are the same, but the geopolymer concrete makes the geopolymer bonds but the alkali-activated concrete makes the C-S-H bonds, and it is the same bond constructed by the Portland cement in the geopolymer bond formation of silica and alumina bonds $(Al - O - Si - O)_n$. In the geopolymer concrete, all constituents have their unique importance. The pozzolanic materials are industrial solid wastes that reduce the waste storage area and reduce the pollution developing due to waste management and Portland cement production. The sodium hydroxide and sodium silicate work as catalysts to activate pozzolans to react and make bonds. A superplasticiser is used to make the concrete workable at less water content.

Nowadays, the predictions of the mechanical strength of the geopolymer concrete are performed by the use of machine learning methods like ANN (artificial neural network), GEP (gene expression programming), multiple linear regression, generalized linear modelling, quadratic polynomial regression, support vector machine, random forest, and extreme gradient boosting [39–46]. The mechanical strength (compressive strength, splitting tensile, and flexural strength) would vary with the variation in the constituent's material quantity. Machine learning methods develop a model to predict the compressive strength and other strengths on the basis of the quantity of the constituent material [47, 48]. The numerical models are developed by the machine learning methods, and the performance of the developed model is analysed by the R^2 value [49–52]. If it is near 1, then the numerical models provide higher accuracy in the prediction of strength [53].

2. Research Significance

The geopolymer concrete samples were cast in the laboratories and get the mechanical (compressive, splitting tensile, flexural) strength via experimental analysis. The research significance of this study is to predict the mechanical strength of the geopolymer concrete by the use of artificial neural networks and random forest algorithm machine learning methods. The predicted values are validated by the experimental results, and we check the accuracy of the prediction of the results. The numerical models are developed by the ANN and random tree methods separately. The predicted result performance was evaluated by the R^2, MAE (mean square error), RMSE (root mean square error), RAE (relative absolute error), and RRSE (root-relative square error).

3. Experimental Programme

3.1. Materials. In the geopolymer concrete mix, the GGBFS and fly ash were used as binding materials, whereas sodium hydroxide and sodium silicate are used as alkaline solutions. The coarse aggregates of 20 mm are used as maximum size aggregates, and the stone dust or m-sand is used as fine aggregates in the GPC. The SNF-based SP Conplast 430 is used as a superplasticiser in the GPC. SEM analysis was conducted on the fly ash and GGBFS, which clarified that the fly ash is spherical and porous, whereas the GGBFS particles are irregular in nature. Table 1 depicts the mineral oxides present in the fly ash and GGBFS. Sodium hydroxide and sodium silicate were purchased from CDH Chemicals Private Limited, in which sodium hydroxide flakes have 98 percent of the minimum assay, whereas sodium silicates are alkaline in nature. Coarse aggregate and fine aggregates were collected from the locally available materials. Various tests were conducted on the coarse and fine aggregates to check their properties that meet the standards [49–52, 54–58]. Table 2 describes the properties of the fine aggregates

TABLE 1: Mineral composition of GGBFS and fly ash.

Characteristics	SiO_2	Al_2O_3	CaO	Fe_2O_3	MgO	SO_3	LOI
Fly ash (%)	45.8	21.4	13.7	12.6	1.3	1.9	0.1
GGBFS (%)	34.52	20.66	32.43	0.57	10.09	0.77	0.3

TABLE 2: Properties of fine aggregate/stone dust (m-sand).

Test	Results
Zone	Zone II
Grade	Well graded
Fineness modulus	2.756 (medium sand)
Specific gravity	2.62
Water absorption	1.21%
Silt content	6%
Bulk density	1610 kg/m^3

TABLE 3: Properties of the coarse aggregate.

Test	Results
Fineness modulus	7.29
Specific gravity	2.79
Water absorption	0.2%
Crushing value	23%
Impact value	22%
Flakiness index	24%
Elongation index	30%
Abrasion value	8%

that are found in the laboratory test analysis. Table 3 depicts the properties of the coarse aggregates that are found through the experiment tests conducted in the laboratories. After the laboratory's tests, it is concluded that the coarse and fine aggregates are suitable for further investigation. Tap water is used in the mixing of geopolymer concrete that has a pH value of 7 [59].

3.2. Synthesis. Table 4 depicts the 10 mix designs of the geopolymer concrete, in which the GGBFS to fly ash ratio varies from 0 to 0.75 as binding materials, and after, the extra water varies from 5% to 30% of the binder. Sodium and sodium silicate solutions were made 20-24 hours before mixing and casting the samples. The pan mixer was used for the mixing of geopolymer concrete for 15 minutes [60]. After the mixing, the slump test was conducted on the mix to find their workability. The fresh mix geopolymer concrete was cast in the cubes, cylinders, and prism moulds of 150 mm × 150 mm × 150 mm, 150 mm × 300 mm, and 100 mm × 100 mm × 500 mm, respectively, for the sample preparation [61–63]. The casted samples were demoulded after three days. The samples were cured in the oven at 60°C for 24 hours after demoulding.

3.3. Experimental Test Setup. The mixed design specimens were tested to find the compressive strength, splitting tensile strength, and flexural tensile strength. All mix design samples were tested after 7 days, 14 days, 28 days, 42 days, and 56 days of casting. Cube samples were used to find compressive strength, cylindrical specimens were used to splitting tensile, and prism shape specimens were used for flexural strength. Cube samples were weighed after 28 of casting, which calculates the density of the samples.

4. Modelling

Two machine learning methods were used to model: artificial neural networks (ANN) and random forest.

4.1. ANN (Artificial Neural Network). ANN architecture is primarily composed of the following elements: the inputs, the weights, the sum function, the activation function, and the outputs. In the ANN work areas, the weights modify the input signals, which are summed with the bias term as shown in equation (1). One of the most important features of an ANN design is its sum function, which is comprised of the inputs and weights [46]. The ANN operates in the following ways. The input signals are changed by the weights, and the modified signals, combined with the bias term, are summed together as shown in

$$ y = f\left(\sum_{i=0}^{n} x_i w_i - b\right), \tag{1} $$

where "f" represents the activation function and the x_i weight of the ith input neuron n represents the number of neurons, and b is the bias term, with the result being denoted as y; the output of the neural network (equation (1)) includes an input for the activation function "f," which is referred to as "sum" in the equation. Multiple feedforward artificial neural networks (ANN) use sigmoid functions, which are mathematical functions having "S"-shaped curves, to activate the network's layers. When we look at equation (2), the variable $\propto$ serves as a constant for controlling gradient in the semilinear zone.

$$ f(t) = \frac{1}{1+e^{-\propto t}}, \quad \text{where } t = \sum_{i=0}^{n} x_i w_i - b. \tag{2} $$

The signals are sent to the next layers of the network until the required outputs are attained. If the computed output differs from the desired goal, the error is calculated and the error is propagated backwards through the network from the output layer to the input layer. The weights are adjusted in response to the signal that has been reflected back. The errors of the output nodes are propagated to all of the nodes of the hidden layers, resulting in each node in the hidden layers being given "blame" for the mistake that occurred.

To produce an accurate forecast of the intended output, the ANN (artificial neural network) must be trained. Normally, data would be divided into two categories: training and testing. The coefficient of determination (R^2), mean

TABLE 4: Mix designs.

Mix designs	Fly ash (kg/m^3)	GGBFS (kg/m^3)	Coarse aggregate (kg/m^3)	Fine aggregate (kg/m^3)	NaOH solution (kg/m^3)	Sodium silicate (kg/m^3)	Superplasticiser (kg/m^3)	Extra water (kg/m^3)
M1	405	—	1269	683	81.0 (13 M)	81.0	—	81
M2	303.75	101.25	1269	683	81.0 (13 M)	81.0	—	81
M3	202.5	202.5	1269	683	81.0 (13 M)	81.0	—	81
M4	101.25	303.75	1269	683	81.0 (13 M)	81.0	—	81
M5	303.75	101.25	1269	683	81.0 (13 M)	81.0	—	0
M6	303.75	101.25	1269	683	81.0 (13 M)	81.0	—	20.25
M7	303.75	101.25	1269	683	81.0 (13 M)	81.0	—	40.5
M8	303.75	101.25	1269	683	81.0 (13 M)	81.0	—	60.75
M9	303.75	101.25	1269	683	81.0 (13 M)	81.0	—	101.25
M10	303.75	101.25	1269	683	81.0 (13 M)	81.0	—	121.5

absolute error (MAE), root mean square error (RMSE), relative absolute error (RAE), and root-relative square error (RRSE) may be used to assess the accuracy of the ANN created in predicting the intended output of the test data.

4.2. Random Forest Tree Algorithm. Random forests are a type of tree predictor in which the values of a random vector gathered independently and with the same distribution for all trees in the forest are used to forecast each tree's behaviour. The generalisation error converges a.s. to a limit as the number of trees in a forest grows bigger. The generalisation error of a forest of tree classifiers is determined by the strength of individual trees in the forest and their association. The error rates are equivalent to AdaBoost when a random selection of features is employed to split each node, but they are more robust in terms of noise. Internal estimates are used to assess error, strength, and correlation as a response to increasing the number of features utilised in the splitting. Internal estimations are also used to establish whether or not variables are important. These ideas can be applied to regression as well. For predicting, random forests are a useful tool. The law of large numbers prevents them from overfitting. When the right kind of randomness is supplied, they become accurate classifiers and regressors. In addition, the framework sheds light on the random forest's forecasting capacity in terms of the strength of individual predictors and their relationships. Using out-of-bag estimates, the otherwise theoretical values of strength and correlation become concrete [64].

5. Results and Discussion

This section describes the experimental results and predicted results via machine learning methods and validates them together.

5.1. Experimental Results. The experimental section describes the slump, density, compressive strength, splitting tensile strength, and flexural strength of the all-mix designs. Slump tests were conducted before the casting of moulds of the plastic mix of the GPC. The density of the design mix of the GPC was calculated after the 28 days of the casting by

the weight of the cube specimens before the compressive strength test. The mechanical strength including compressive strength, splitting tensile strength, and flexural strength was tested after 7 days, 14 days, 28 days, 42 days, and 56 days of the GPC mix casting. All the mechanical properties vary similarly with the mixed design. After 28 days, the compressive strength and all other strengths gained 95 percent strength of total strength. The mechanical strength varied from the ratio of GGBFS to fly ash from 0.00 to 0.75 and got the optimum point at a 0.25 ratio mix. The GPC mix varied the extra water from 5% to 30% of binder content. The optimum point of the mechanical properties was found at 20% of the binder content. The maximum compressive strength, splitting tensile, and flexural strength are 32.9 MPa, 4.8 MPa, and 5.3 MPa, respectively, after 56 days of casting. Tables 5–7 depict the compressive strength, splitting tensile strength, and flexural strength values found after the experimental tests.

5.2. Modelling Analysis. In the modelling analysis, ANN and random forest algorithm machine learning methods are used for the prediction of compressive strength, splitting tensile strength, and flexural strength. Figure 1 shows the working flow chart of the regression model. It shows the total process of the regression work. It starts with data collection which includes the input and output data with their variables. After that, it shows the data preparation for training and testing separately. The training data process the input data with their parameters and classify them. After the completion of training, data were tested with the other remaining datasets. After the completion of training, testing of the data validates the results as output.

5.2.1. ANN Result Analysis. Artificial neural networks are becoming more popular because they could be used to solve a broad variety of problems in science and engineering. Predictive statistical models of complex processes that are nonlinear in nature, such as biological systems, are often employed in this technique. It is possible to simulate a broad spectrum of complex system behaviour with the help of an ANN. Neuron components are used to describe the ANN's functioning, which is much more like a normal human

TABLE 5: Compressive strength in MPa.

Mix designs	7 days	14 days	28 days	42 days	56 days
M1	21.5	25.4	28.3	28.7	29.0
M2	24.4	29.1	32.1	32.6	32.9
M3	22.9	26.4	29.6	30	30.2
M4	21.7	25.1	28.4	29.0	29.3
M5	16.2	18.1	19.9	20.3	20.8
M6	21.3	23.8	26.9	27.3	27.7
M7	23.6	27.6	30.8	31.2	31.6
M8	24.1	28.9	31.9	32.4	32.6
M9	24.0	28.4	31.6	32.0	32.4
M10	23.4	27.6	30.2	30.8	31.1

TABLE 6: Splitting tensile strength in MPa.

Mix designs	7 days	14 days	28 days	42 days	56 days
M1	2.3	2.8	3.1	3.2	3.2
M2	2.9	3.8	4.6	4.7	4.8
M3	2.7	3.6	4.3	4.5	4.6
M4	2.6	3.4	3.9	4.1	4.2
M5	1.9	2.2	2.8	2.9	3.0
M6	2.2	2.9	3.6	3.8	3.9
M7	2.6	3.4	4.0	4.2	4.3
M8	2.8	3.8	4.4	4.6	4.7
M9	2.7	3.6	4.3	4.5	4.6
M10	2.5	3.2	3.9	4.2	4.3

TABLE 7: Flexural strength in MPa.

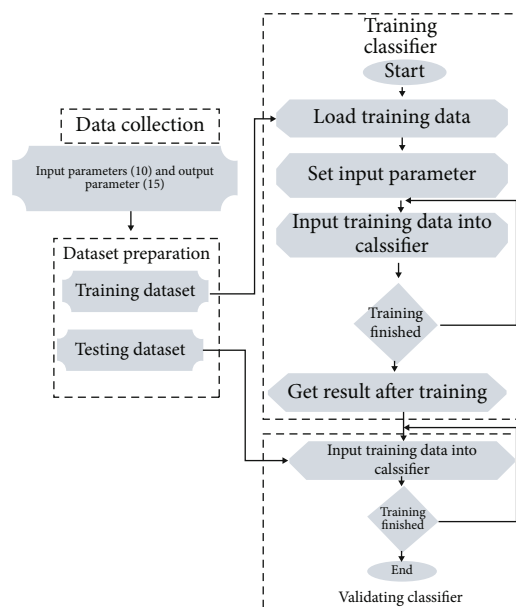| Mix designs	7 days	14 days	28 days	42 days	56 days
M1	2.5	3.0	3.5	3.6	3.6
M2	3.1	4.0	5.0	5.2	5.3
M3	2.9	3.7	4.5	4.7	4.9
M4	2.7	3.6	4.2	4.4	4.6
M5	2.1	2.4	3.0	3.2	3.3
M6	2.5	3.1	3.7	3.9	4.0
M7	2.8	3.5	4.2	4.4	4.5
M8	3.0	3.8	4.6	4.7	4.8
M9	2.9	3.6	4.4	4.6	4.7
M10	2.7	3.2	4.0	4.2	4.3

FIGURE 1: Regression working flow chart.

input layer, the hidden layers, and the output layer. Before data training, the input and output layers are defined, and the hidden layer on the other hand is discovered by trial and error during data training. Figure 2 represents a common ANN architectural model. It describes the initially put input of 10 datasets of 10-attribute numeric type and after applying the regression method multilayer perception on that. After the input is applied, target the 15 classes.

The model is composed of input factors $(x_1, x_2, x_3, x_4 \cdots x_n)$ and weights $(w_1, w_2, w_3, w_4 \cdots w_n)$, with weights $(y_1, y_2, y_3, y_4 \cdots y_n)$ for each factor. Singular value or sum function (sigmoid) processing is the ultimate processing method, and it has the final impact on the outputs. As a result, equation (1) provides a broad description of the analogy.

It has been shown in the study that the ANN technique is capable of anticipating significant responses regardless of whether the data being processed is riddled with errors or missing information. The ANN method is divided into three stages which are learning, training, and model performance evaluation. The first of these efforts is education. The output variables are predicted correctly during the training stage, and the network's weights and biases (supervised or unsupervised) are modified to ensure that the output variables are predicted reliably. The supervised training approach constructs a model using previously completed experimental data, while the unsupervised training method does not employ real-world input and output data. During the testing stage, the network may react to the input without modifying the overall network architecture.

After a series of trials and errors, the best ANN model may be found at the end of each stage of development. At some point in the learning process, Alshihri realized that it was feasible to continue developing a large number of networks, at which time the process could be paused and evaluated at various points in the learning process. Use

brain. To put it another way, "garbage in and garbage out" refers to a way of computer works, as input parameters are used to duplicate the system's process in order to decide the output. To build an ANN model, the input and output components must be included with the latter being controlled by the former. The ANN principle is made up of a network of interconnected neurons, each of which carries its own weight. This means that the model's answer is found by multiplying the weight by the network's total number of signals. There are three layers in a basic ANN network: the
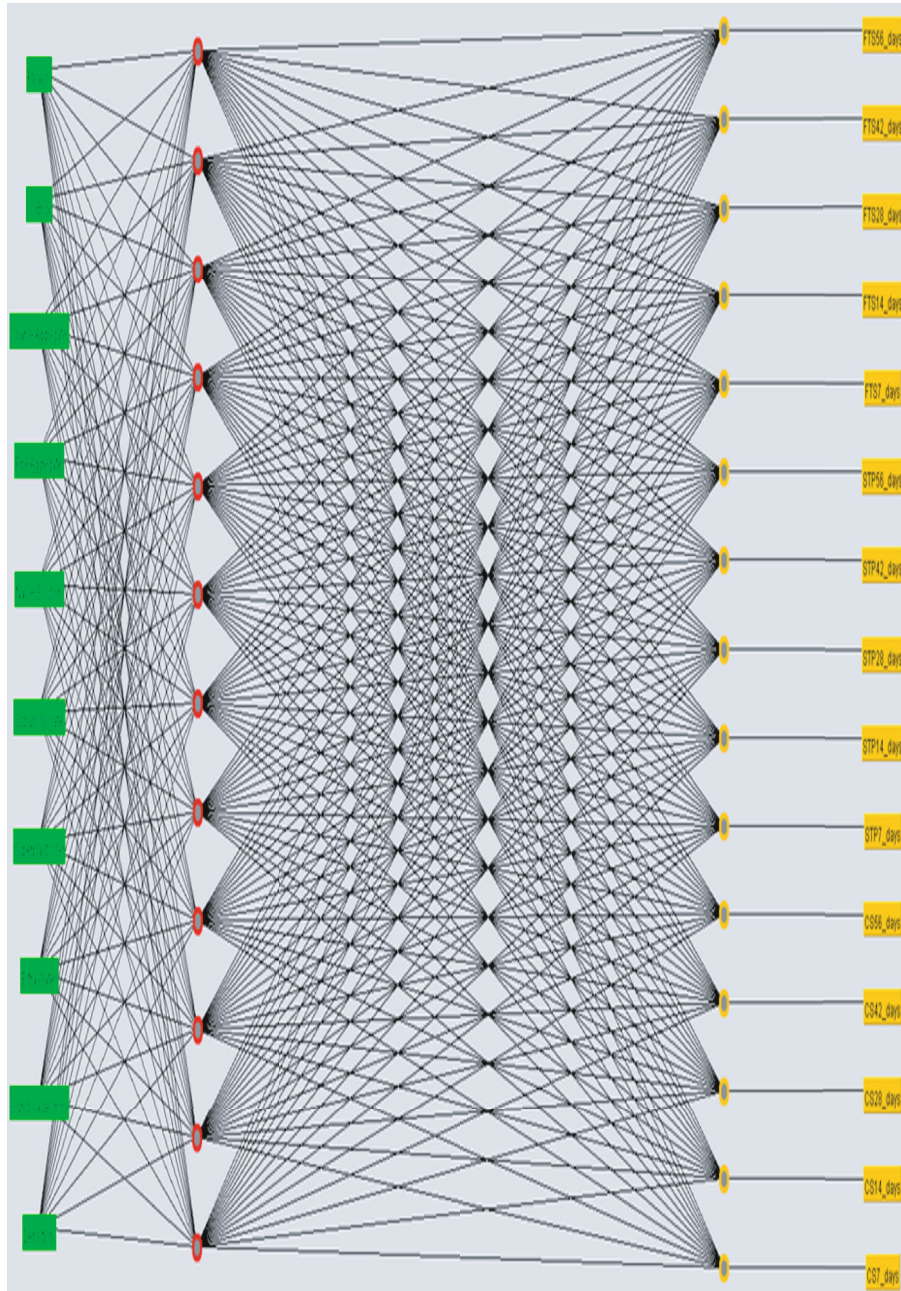
FIGURE 2: ANN architecture that best models the performance of the geopolymer concrete.

different random weights to reexamine the network, and keep going until you get the results you want. When it comes to selecting the best neural network model, R^2 (result coefficient) and MSE (mean square error) are the most important metrics to consider. MATLAB software was used to evaluate the ANN model's performance. The straining and recall techniques were used to build the model utilizing the error backpropagation approach. Lee claims that this approach can deal with issues involving several variables (multidimensional). Table 8 shows the datasets that were used for model development in this study. An LM multilayer feedforward backpropagation model was used to train the data, which is easily accessible in the MATLAB computing environment and is based on the feedforward backpropagation model. A total of 250 samples of data (including those from this study and others like it) were used to compile the database for this study's findings. Seventy percent of the input data was utilized in the learning phase, and fifteen percent was used in each of the testing and validation stages. The data in MATLAB were automatically normalized rather than manually dividing using the maximum values, which was done by hand in MATLAB. The procedure was done multiple times until the best model that met the R^2 and MSE conditions was found.

Geopolymer concrete's compressive strength, splitting tensile strength, and flexural strength may be calculated by

TABLE 8: Input and output specification for the model development.

Input data		Minimum	Maximum
Fly ash (kg/m^3)		405	101.25
GGBFS (kg/m^3)		0	303.75
Extra water (kg/m^3)		0	121.5
Slump (mm)		0	190
Density (kg/m^3)		2406	2506
Coarse aggregate (kg/m^3)		1269	1269
Fine aggregate (kg/m^3)		683	683
NaOH solution (kg/m^3)		81	81
Sodium silicate (kg/m^3)		81	81
Superplasticiser (kg/m^3)		4.05	4.05
Output data			
	7 days	16.2	24.4
	14 days	18.1	29.1
Compressive strength (MPa)	28 days	19.9	32.1
	42 days	20.3	32.6
	56 days	20.8	32.9
	7 days	1.9	2.9
	14 days	2.2	3.8
Splitting tensile (MPa)	28 days	2.8	4.6
	42 days	2.9	4.7
	56 days	3	4.8
	7 days	2.1	3.1
	14 days	2.4	4
Flexural strength (MPa)	28 days	3	5
	42 days	3.2	5.2
	56 days	3.3	5.3

$$R^2 = \frac{\left(n\sum x_i y_i - \sum x_i \sum y_i\right)^2}{\left(n\sum x_i^2 - \left(\sum x_i\right)^2\right)\left(n\sum y_i^2 - \left(\sum y_i\right)^2\right)},$$

$$\text{MAE} = \frac{1}{n}\sum_{i=1}^{n}|x_i - y_i|,$$

$$\text{RMSE} = \sqrt{\left(\frac{1}{n}\right)\sum_{i=1}^{n}|x_i - y_i|^2}, \qquad (3)$$

$$\text{RAE} = \frac{\sum_{i=1}^{n}|x_i - y_i|}{\sum_{i=1}^{n}|x_i - (1/n)\sum_{i=1}^{n}x_i|},$$

$$\text{RRSE} = \sqrt{\frac{\sum_{i=1}^{n}(x_i - y_i)^2}{\sum_{i=1}^{n}(x_i - (1/n)\sum_{i=1}^{n}x_i)^2}},$$

where "x" represents the experimental value, "y" represents the predicted value, and "n" represents the total number of values.

As shown by the chosen network architecture's performance, the projected and actual testing results on geopolymer concrete are highly compatible. While maintaining a high degree of accuracy in its predictions, the chosen model can provide both input and output data for the tested concrete. A low matching percent error for the anticipated strength further supports the model's usefulness, indicating that the prediction made by this model is statistically reliable. This conclusion shows that the model's performance may be relied on in absolute terms because of the proximity of the datasets (predicted and actual). This demonstrates that the selected model is capable of accurately responding to a system with a high degree of confidence in its performance. Tables 12, 13, and 14 show the validation of results between actual and predicted values by both the ANN model and the random tree method. Tables 9, 10, and 11 show the performance of the machine learning method model for the prediction of mechanical strength to the actual results found through experimental analysis.

5.2.2. Random Forest Results. We provide a simple and effective random forest in this study. It is executed on the server to process the data collected from the input. The random forest algorithm illustrates the suggested model's definition and process flow, respectively. Table 12 shows the validation between the compressive strength of actual output vs. predicted output by both ANN and random tree. Table 9 shows the performance of prediction with their limited error of compressive strength. Similarly, Tables 13 and 14 show validation of splitting tensile and flexural strength between actual experimental and predicted values. Tables 10 and 11 show the performance of prediction with their limited error of splitting tensile and flexural strength.

Table 12 describes the compressive strength value at 7 days, 14 days, 28 days, 42 days, and 56 days, which includes the actual value and predicted value. ANN and random forest tree machine learning methods were used to predict the compressive strength. The random forest tree method predicted a more accurate compressive strength than the

using an empirical model. Input data of the geopolymer concrete that was formed included fly ash and GGBS as well as extra water, slump value, density, sodium hydroxide, sodium silicate, coarse and fine particles, and superplasticiser. The output data included the kind of concrete produced and the type of concrete produced. The most important output variables are compression strength, split tensile strength, and flexural strength. Various testing periods of 7, 14, 28, 42, and 56 days were included in the output data (age). To achieve the lowest feasible mean squared error (MSE), the ANN architecture shown in Figure 2 has been optimized to represent the concrete's behaviour. An estimated ten neurons are found in the input phase, twelve are in the hidden layer, and fifteen are in the output layer. For the selected model, the correlation and error analysis results are shown in Tables 9, 10, and 11. Results in Tables 5, 6, and 7 show that the model selected fits the criterion for error performance in a neural network model of artificial intelligence. In the case when a model's R^2 is near one and its MSE is modest, it shows that the predicted and actual data are perfectly correlated. When it comes to ANN models, it is widely accepted that the better the model, the better it is in foretelling the future behaviour of a system. Errors were calculated by using the following mathematical formulas to determine the R^2, MAE, RMSE, RAE, and RRSE:

TABLE 9: Compressive strength performance analysis evaluation between actual experimental results and predicted results.

| | 7 days | | 14 days | | 28 days | | 42 days | | 56 days | |
	Random tree	ANN	Random tree	ANN	Random tree	ANN	Random tree	ANN	Random tree	ANN
R^2	1	0.9992	1	0.9997	0.9999	0.9982	0.9999	0.999	1	0.9984
MAE	0	0.0886	0	0.0739	0.02	0.2593	0.02	0.1943	0	0.258
RMSE	0	0.1146	0	0.104	0.0447	0.3193	0.0447	0.2374	0	0.3088
RAE	0	5.19%	0%	3.14%	0.81%	10.47%	0.81%	7.82%	0%	10.54%
RRSE	0	4.98%	0%	3.33%	1.30%	9.30%	1.29%	6.87%	0%	9.08%

TABLE 10: Splitting tensile strength performance analysis evaluation between actual experimental results and predicted results.

| | 7 days | | 14 days | | 28 days | | 42 days | | 56 days | |
	Random tree	ANN	Random tree	ANN	Random tree	ANN	Random tree	ANN	Random tree	ANN
R^2	1	0.9994	1	0.9978	1	0.9991	1	0.9984	1	0.9983
MAE	0	0.0108	0	0.0333	0	0.0267	0	0.0359	0	0.0363
RMSE	0	0.013	0	0.0459	0	0.0356	0	0.0484	0	0.05
RAE	0	4.56%	0	8.40%	0	6.15%	0	7.77%	0	7.63%
RRSE	0	4.50%	0	9.52%	0	6.50%	0	8.44%	0	8.49%

TABLE 11: Flexural tensile strength performance analysis evaluation between actual experimental results and predicted results.

| | 7 days | | 14 days | | 28 days | | 42 days | | 56 days | |
	Random tree	ANN	Random tree	ANN	Random tree	ANN	Random tree	ANN	Random tree	ANN
R^2	1	0.9985	1	0.9989	1	0.9987	1	0.9998	1	0.9999
MAE	0	0.0159	0	0.0188	0	0.0319	0	0.0144	0	0.0114
RMSE	0	0.0185	0	0.0269	0	0.0423	0	0.0188	0	0.0149
RAE	0	7.25%	0	5.05%	0	7.13%	0	3.18%	0	2.38%
RRSE	0	6.64%	0	6.03%	0	7.64%	0	3.38%	0	2.56%

TABLE 12: Compressive strength validation between actual experimental results and predicted results.

| | 7 days | | | 14 days | | | 28 days | | | 42 days | | | 56 days | | |
| | | Predicted | | | Predicted | | | Predicted | | | Predicted | | | Predicted | |
Actual	Random tree	ANN	Actual	Random tree	ANN	Actual	Random tree	ANN	Actual	Random tree	ANN	Actual	Random tree	ANN
21.5	21.5	21.48	25.4	25.4	25.388	28.3	28.3	28.265	28.7	28.7	28.671	29	29	28.959
24.4	24.4	24.173	29.1	29.1	28.955	32.1	32	31.822	32.6	32.5	32.361	32.9	32.9	32.599
22.9	22.9	22.904	26.4	26.4	26.367	29.6	29.6	29.393	30	30	29	30.2	30.2	29.926
21.7	21.7	21.538	25.1	25.1	24.882	28.4	28.4	27.806	29	29	28.546	29.3	29.3	28.77
16.2	16.2	16.204	18.1	18.1	18.111	19.9	19.9	19.928	20.3	20.3	20.338	20.8	20.8	20.834
21.3	21.3	21.177	23.8	23.8	23.653	26.9	26.9	26.478	27.3	27.3	26.97	27.7	27.7	27.308
23.6	23.6	23.47	27.6	27.6	27.477	30.8	30.8	30.42	31.2	31.2	30.937	31.6	31.6	31.204
24.1	24.1	24.19	28.9	28.9	28.939	31.9	32	31.959	32.4	32.5	32.452	32.6	32.6	32.683
24	24	23.886	28.4	28.4	28.401	31.6	31.6	31.156	32	32	31.714	32.4	32.4	31.982
23.4	23.4	23.387	27.6	27.6	27.588	30.2	30.2	30.052	30.8	30.8	30.716	31.1	31.1	30.99

ANN method. Ten data are used at the same time for individual compressive strength. This table contains the 150 datasets of the compressive strength, whereas the actual data are 50 and the predicted data are 100.

The analysis, known as the sensitivity analysis, was conducted to determine the impact of each variable on the prediction of the mechanical strength of GPC. It is important to understand how each of the input parameters will

TABLE 13: Splitting tensile strength validation between actual experimental results and predicted results.

| | 7 days | | | 14 days | | | 28 days | | | 42 days | | | 56 days | |
| | Predicted | | | Predicted | | | Predicted | | | Predicted | | | Predicted | |
Actual	Random tree	ANN	Actual	Random tree	ANN	Actual	Random tree	ANN	Actual	Random tree	ANN	Actual	Random tree	ANN
2.3	2.3	2.297	2.8	2.8	2.802	3.1	3.1	3.103	3.2	3.2	3.204	3.2	3.2	3.203
2.9	2.9	2.876	3.8	3.8	3.814	4.6	4.6	4.615	4.7	4.7	4.716	4.8	4.8	4.811
2.7	2.7	2.693	3.6	3.6	3.647	4.3	4.3	4.332	4.5	4.5	4.542	4.6	4.6	4.641
2.6	2.6	2.588	3.4	3.4	3.445	3.9	3.9	3.943	4.1	4.1	4.162	4.2	4.2	4.266
1.9	1.9	1.899	2.2	2.2	2.22	2.8	2.8	2.815	2.9	2.9	2.92	3	3	3.022
2.2	2.2	2.183	2.9	2.9	2.974	3.6	3.6	3.642	3.8	3.8	3.854	3.9	3.9	3.955
2.6	2.6	2.581	3.4	3.4	3.502	4	4	4.083	4.2	4.2	4.314	4.3	4.3	4.419
2.8	2.8	2.809	3.8	3.8	3.797	4.4	4.4	4.399	4.6	4.6	4.598	4.7	4.7	4.699
2.7	2.7	2.686	3.6	3.6	3.613	4.3	4.3	4.327	4.5	4.5	4.532	4.6	4.6	4.63
2.5	2.5	2.502	3.2	3.2	3.213	3.9	3.9	3.907	4.2	4.2	4.213	4.3	4.3	4.316

TABLE 14: Flexural strength validation between actual experimental results and predicted results.

| | 7 days | | | 14 days | | | 28 days | | | 42 days | | | 56 days | |
| | Predicted | | | Predicted | | | Predicted | | | Predicted | | | Predicted | |
Actual	Random tree	ANN	Actual	Random tree	ANN	Actual	Random tree	ANN	Actual	Random tree	ANN	Actual	Random tree	ANN
2.5	2.5	2.498	3	3	3.002	3.5	3.5	3.505	3.6	3.6	3.602	3.6	3.6	3.602
3.1	3.1	3.074	4	4	4.014	5	5	5.028	5.2	5.2	5.215	5.3	5.3	5.312
2.9	2.9	2.912	3.7	3.7	3.728	4.5	4.5	4.54	4.7	4.7	4.719	4.9	4.9	4.914
2.7	2.7	2.718	3.6	3.6	3.621	4.2	4.2	4.238	4.4	4.4	4.415	4.6	4.6	4.613
2.1	2.1	2.111	2.4	2.4	2.412	3	3	3.016	3.2	3.2	3.206	3.3	3.3	3.305
2.5	2.5	2.521	3.1	3.1	3.12	3.7	3.7	3.762	3.9	3.9	3.928	4	4	4.022
2.8	2.8	2.837	3.5	3.5	3.572	4.2	4.2	4.295	4.4	4.4	4.442	4.5	4.5	4.533
3	3	3.012	3.8	3.8	3.789	4.6	4.6	4.599	4.7	4.7	4.7	4.8	4.8	4.8
2.9	2.9	2.909	3.6	3.6	3.602	4.4	4.4	4.43	4.6	4.6	4.614	4.7	4.7	4.712
2.7	2.7	2.711	3.2	3.2	3.207	4	4	4.005	4.2	4.2	4.203	4.3	4.3	4.302

affect the projected outcome because they are crucial to the accuracy of the models that are used for prediction. Each input parameter contributed to the predicted output of the mechanical strength of GPC.

Table 9 depicts the coefficient of determination (R^2), mean absolute error (MAE), root mean square error (RMSE), relative absolute error (RAE), and root-relative square error (RRSE) values of predicted compressive strength to the actual experimental results of both machine learning methods. The random forest tree model is more relevant to the ANN model in all-day compressive strength. The random forest tree method shows a determination coefficient value of 1 at 7 days, 14 days, and 56 days, whereas the ANN model does not show a determination coefficient value of 1 in any day prediction.

Table 13 describes the splitting tensile strength value at 7 days, 14 days, 28 days, 42 days, and 56 days, which includes the actual value and predicted value. ANN and random forest tree machine learning methods were used to predict the splitting tensile. The random forest tree method predicted more accurate splitting tensile strength than the

ANN method. Ten data are used at the same time for individual compressive strength. This table contains the 150 datasets of the compressive strength, whereas the actual data are 50 and the predicted data are 100.

Table 10 depicts the coefficient of determination (R^2), mean absolute error (MAE), root mean square error (RMSE), relative absolute error (RAE), and root-relative square error (RRSE) values of predicted splitting tensile strength to the actual experimental results of both machine learning methods. The random forest tree model is more relevant to the ANN model in all-day splitting tensile strength. The random forest tree method shows a determination coefficient value of 1 at 7 days, 14 days, 28 days, 42 days, and 56 days, whereas the ANN model does not show a determination coefficient value of 1 in any day prediction.

Table 14 describes the flexural strength value at 7 days, 14 days, 28 days, 42 days, and 56 days, which includes the actual value and predicted value. ANN and random forest tree machine learning methods were used to predict flexural strength. The random forest tree method predicted more accurate flexural strength than the ANN method. Ten data

are used at the same time for individual compressive strength. This table contains the 150 datasets of the compressive strength, whereas the actual data are 50 and the predicted data are 100.

Table 11 depicts the coefficient of determination (R^2), mean absolute error (MAE), root mean square error (RMSE), relative absolute error (RAE), and root-relative square error (RRSE) values of predicted flexural tensile strength to the actual experimental results of both machine learning methods. The random forest tree model is more relevant to the ANN model in all-day flexural strength. The random forest tree method shows a determination coefficient value of 1 at 7 days, 14 days, 28 days, 42 days, and 56 days, whereas the ANN model does not show a determination coefficient value of 1 in any day prediction.

6. Conclusion

After the experimental investigation, we found the results of the mechanical strength. The machine learning methods ANN and random forest develop the models based on experimental inputs and outputs. Conclusion is based on the following areas:

(i) In the experimental analysis, the M2 mix got the maximum mechanical (including compressive, splitting tensile, and flexural tensile) strengths whereas the M5 mix gets the minimum mechanical strengths among all the mix designs

(ii) ANN and random forest models check the performance of prediction based on the R^2, MAE, RMSE, RAE, and RRSE

(iii) Random forest models show the best prediction to the ANN models because it shows the negligible error between actual and predicted values. The R^2 value is 1 of 12 predicted results out of 15 by the use of random forest methods. So it is most suitable to predict the strength of geopolymer concrete based on their constituent's material quantity

Data Availability

All data are made available in the manuscript.

Conflicts of Interest

There are no conflicts of interest in this article.

Acknowledgments

References

[1] B. Sabir, S. Wild, and J. Bai, "Metakaolin and calcined clays as pozzolans for concrete: a review," *Cement and Concrete Composites*, vol. 23, no. 6, pp. 441–454, 2001.

[2] S. Dadsetan, H. Siad, M. Lachemi, and M. Sahmaran, "Construction and demolition waste in geopolymer concrete technology: a review," *Magazine of Concrete Research*, vol. 71, no. 23, pp. 1232–1252, 2019.

[3] D. Bondar, C. J. Lynsdale, N. B. Milestone, and N. Hassani, "Sulfate resistance of alkali activated pozzolans," *Int. J. Concr. Struct. Mater.*, vol. 9, no. 2, pp. 145–158, 2015.

[4] D. Bondar, C. J. Lynsdale, N. B. Milestone, N. Hassani, and A. A. Ramezanianpour, "Engineering properties of alkali activated natural pozzolan concrete," *ACI Materials Journal*, vol. 108, no. 1, pp. 64–72, 2010.

[5] S. A. Ishak and H. Hashim, "Low carbon measures for cement plant - a review," *Journal of Cleaner Production*, vol. 103, pp. 260–274, 2015.

[6] R. Priyanka, R. Selvaraj, and B. Rajesh, "Characterisation study on clay based geopolymer concrete," *International Journal of Engineering and Applied Sciences*, vol. 5, pp. 49–55, 2015.

[7] C. A. Jeyasehar and M. Salahuddin, *Development of fly ash based geopolymer concrete precast elements*, Ministry of Environment and Forests of India and Annamalai University, 2013.

[8] P. K. Mehta and P. J. M. Monteiro, *Concrete microstructure, Properties, and Materials*, McGraw-Hill Education, 2014.

[9] F. Pacheco-Torgal, Z. Abdollahnejad, S. Miraldo, S. Baklouti, and Y. Ding, "An overview on the potential of geopolymers for concrete infrastructure rehabilitation," *Construction and Building Materials*, vol. 36, pp. 1053–1058, 2012.

[10] M. Verma, N. Dev, I. Rahman, M. Nigam, M. Ahmed, and J. Mallick, "Geopolymer concrete : a material for sustainable development in Indian construction industries," *Crystals*, vol. 12, no. 4, p. 514, 2022.

[11] M. Verma and N. Dev, "Review on the effect of different parameters on behavior of geopolymer concrete," *International Journal of Innovative Research in Science, Engineering and Technology*, vol. 6, pp. 11276–11281, 2017.

[12] M. Verma and N. Dev, "Geopolymer concrete : a way of sustainable construction," *International Journal of Recent Research Aspects*, vol. 5, pp. 201–205, 2018.

[13] R. Kumar, M. Verma, and N. Dev, "Investigation on the effect of seawater condition, sulphate attack, acid attack, freeze-thaw condition, and wetting–drying on the geopolymer concrete," *Iranian Journal of Science and Technology, Transactions of Civil Engineering*, vol. 45, pp. 1–31, 2021.

[14] M. Verma and N. Dev, "Effect of liquid to binder ratio and curing temperature on the engineering properties of the geopolymer concrete," *SILICON*, vol. 14, no. 4, pp. 1743–1757, 2022.

[15] M. Verma and N. Dev, "Effect of ground granulated blast furnace slag and fly ash ratio and the curing conditions on the mechanical properties of geopolymer concrete," in *Structural Concrete*, pp. 1–15, Wiley, 2021.

[16] M. Verma and M. Nigam, "Mechanical behaviour of self compacting and self curing concrete," *International Journal of Innovative Research in Science, Engineering and Technology*, vol. 6, pp. 14361–14366, 2017.

[17] M. Verma and N. Dev, "Sodium hydroxide effect on the mechanical properties of flyash-slag based geopolymer concrete," *Structural Concrete*, vol. 22, no. S1, pp. E368–E379, 2021.

[18] M. Verma and N. Dev, "Effect of SNF-based superplasticizer on physical, mechanical and thermal properties of the geopolymer concrete," *Silicon*, vol. 14, no. 3, pp. 965–975, 2022.

[19] A. Chouksey, M. Verma, N. Dev, I. Rahman, and K. Upreti, "An investigation on the effect of curing conditions on the mechanical and microstructural properties of the geopolymer concrete," *Mater. Res. Express.*, vol. 9, no. 5, article 055003, 2022.

[20] M. Verma, "Experimental investigation on the properties of geopolymer concrete after replacement of river sand with the M-sand," in *International e-Conference on Sustainable Development & Recent Trends in Civil Engineering*, New Delhi, India, 2022.

[21] R. Kumar, M. Verma, and N. Dev, "Investigation of fresh, mechanical, and impact resistance properties of rubberized concrete," in *International e-Conference on Sustainable Development & Recent Trends in Civil Engineering*, pp. 88–94, 2022.

[22] M. Verma and N. Dev, "Effect of superplasticiser on physical, chemical and mechanical properties of the geopolymer concrete," in *Challenges of Resilient and Sustainable Infrastructure Development in Emerging Economies*, pp. 1185–1191, Kolkata, India, 2020.

[23] J. Davidovits, *Geopolymer chemistry and Applications*, J. Davidovits.–Saint-Quentin, France, 5th edition, 2020.

[24] J. Davidovits, "30 years of successes and failures in geopolymer applications. Market trends and potential breakthroughs," in *Geopolymer 2002 Conference*, pp. 1–16, Melbourne, Australia, 2002.

[25] J. Davidovits, "Geopolymers and geopolymeric materials," *Journal of Thermal Analysis*, vol. 35, no. 2, pp. 429–441, 1989.

[26] J. Davidovits and S. Quentin, "Geopolymers," *Journal of Thermal Analysis and Calorimetry*, vol. 37, no. 8, pp. 1633–1656, 1991.

[27] P. Nuaklong, V. Sata, A. Wongsa, K. Srinavin, and P. Chindaprasirt, "Recycled aggregate high calcium fly ash geopolymer concrete with inclusion of OPC and nano-SiO2," *Construction and Building Materials*, vol. 174, pp. 244–252, 2018.

[28] J. Shang, J. G. Dai, T. J. Zhao, S. Y. Guo, P. Zhang, and B. Mu, "Alternation of traditional cement mortars using fly ash-based geopolymer mortars modified by slag," *Journal of Cleaner Production*, vol. 203, pp. 746–756, 2018.

[29] H. Zhang, L. Li, P. K. Sarker et al., "Investigating various factors affecting the long-term compressive strength of heat-cured fly ash geopolymer concrete and the use of orthogonal experimental design method," *Int. J. Concr. Struct. Mater.*, vol. 13, no. 1, 2019.

[30] Y. Cui, P. Zhang, and J. Bao, "Bond stress between steel-reinforced bars and fly ash-based geopolymer concrete," *Advances in Materials Science and Engineering*, vol. 2020, 11 pages, 2020.

[31] H. Y. Zhang, V. Kodur, B. Wu, L. Cao, and F. Wang, "Thermal behavior and mechanical properties of geopolymer mortar after exposure to elevated temperatures," *Construction and Building Materials*, vol. 109, pp. 17–24, 2016.

[32] Y. Liu, Z. Zhang, C. Shi, D. Zhu, N. Li, and Y. Deng, "Development of ultra-high performance geopolymer concrete (UHPGC): influence of steel fiber on mechanical properties," *Cement and Concrete Composites*, vol. 112, article 103670, 2020.

[33] B. Zhang, Æ. K. J. D. Mackenzie, I. W. M. M. Brown, K. J. D. Mac Kenzie, and I. W. M. M. Brown, "Crystalline phase formation in metakaolinite geopolymers activated with NaOH and sodium silicate," *Journal of Materials Science*, vol. 44, no. 17, pp. 4668–4676, 2009.

[34] Y. Zhang, W. Sun, Z. Li, and X. Zhou, "Impact properties of geopolymer based extrudates incorporated with fly ash and PVA short fiber," *Construction and Building Materials*, vol. 22, no. 3, pp. 370–383, 2008.

[35] X. Y. Zhuang, L. Chen, S. Komarneni et al., "Fly ash-based geopolymer: clean production, properties and applications," *Journal of Cleaner Production*, vol. 125, pp. 253–267, 2016.

[36] A. Gupta, N. Gupta, and K. K. Saxena, "Mechanical and durability characteristics assessment of geopolymer composite (GPC) at varying silica fume content," *J. Compos. Sci.*, vol. 5, no. 9, p. 237, 2021.

[37] A. Gupta, N. Gupta, and K. K. Saxena, "Experimental study of the mechanical and durability properties of slag and calcined clay based geopolymer composite," in *Advances in Materials and Processing Technologies*, pp. 1–15, Taylor & Francis, 2021.

[38] A. Arulrajah, T.-A. Kua, C. Phetchuay, S. Horpibulsuk, F. Mahghoolpilehrood, and M. M. Disfani, "Spent coffee grounds–fly ash geopolymer used as an embankment structural fill material," *Journal of Materials in Civil Engineering*, vol. 28, no. 5, 2016.

[39] M. A. Khan, S. A. Memon, F. Farooq, M. F. Javed, F. Aslam, and R. Alyousef, "Compressive strength of fly-ash-based geopolymer concrete by gene expression programming and random forest," *Advances in Civil Engineering*, vol. 2021, Article ID 6618407, 17 pages, 2021.

[40] Q. Wang, W. Ahmad, A. Ahmad, F. Aslam, A. Mohamed, and N. I. Vatin, "Application of soft computing techniques to predict the strength of geopolymer composites," *Polymers*, vol. 14, no. 6, p. 1074, 2022.

[41] P. Gupta, N. Gupta, K. K. Saxena, and S. Goyal, "Random forest modeling for fly ash-calcined clay geopolymer composite strength detection," *J. Compos. Sci.*, vol. 5, no. 10, p. 271, 2021.

[42] A. Ahmad, W. Ahmad, F. Aslam, and P. Joyklad, "Compressive strength prediction of fly ash-based geopolymer concrete via advanced machine learning techniques," *Case Studies in Construction Materials*, vol. 16, article e00840, 2022.

[43] A. Shaqadan, "Prediction of concrete mix strength using random forest model," *International Journal of Applied Engineering Research*, vol. 11, pp. 11024–11029, 2016.

[44] H. V. T. Mai, T. A. Nguyen, H. B. Ly, and V. Q. Tran, "Prediction compressive strength of concrete containing GGBFS using random forest model," *Advances in Civil Engineering*, vol. 2021, Article ID 6671448, 12 pages, 2021.

[45] A. Ahmad, K. A. Ostrowski, M. Maślak, F. Farooq, I. Mehmood, and A. Nafees, "Comparative study of supervised machine learning algorithms for predicting the compressive strength of concrete at high temperature," *Materials (Basel).*, vol. 14, no. 15, 2021.

[46] X. Kong and A. M. Khambadkone, "Modeling of a PEM fuel-cell stack for dynamic and steady-state operation using ANN-based submodels," *IEEE Transactions on Industrial Electronics*, vol. 56, no. 12, pp. 4903–4914, 2009.

[47] R. Haddad and I. Al-Qadi, "Characterization of Portland cement concrete using electromagnetic waves over the microwave frequencies," *Cement and Concrete Research*, vol. 28, no. 10, pp. 1379–1391, 1998.

[48] J. G. J. Olivier, K. M. Schure, and J. A. H. W. Peters, "Trends in global CO2 and total greenhouse gas emissions," *PBL Netherlands Environmental Assessment Agency*, vol. 5, 2017.

[49] IS 2386 (Part I), *Methods of test for aggregates for concrete part I particle size and shape*, vol. 2386, Bureau of Indian Standards, 1997.

[50] IS 2386 (Part VIII), *Methods of test for aggregates for concrete part VIII petrographic examination*, vol. 2386, Bureau of Indian Standards, 1997.

[51] IS 2386 (Part III), *Methods of test for aggregates for concrete part III specific gravity, density, voids, absorption and bulking*, vol. 2386, Bureau of Indian Standards, 1997.

[52] IS 2386 (Part VI), *Methods of test for aggregates for concrete part VI measuring mortar making properties of fine aggregate*, vol. 2386, Bureau of Indian Standards, 1997.

[53] A. Sadrmomtazi, J. Sobhani, and M. A. Mirgozar, "Modeling compressive strength of EPS lightweight concrete using regression, neural network and ANFIS," *Construction and Building Materials*, vol. 42, pp. 205–216, 2013.

[54] M. Kisan, S. Sangathan, J. Nehru, and S. G. Pitroda, "IS 2386 (Part II)," in *Methods of test for aggregates for concrete part II estimation of deleterious materials and organic impurties*, Bureau of Indian Standards, New Delhi, India, 1998.

[55] IS 2386 (Part IV), *Methods of test for aggregates for concrete part IV mechanical properties*, vol. 2386, Bureau of Indian Standards, 1997.

[56] IS 2386 (Part V), *Methods of test for aggregates for concrete part V soundness*, Bureau of Indian Standards, 1997.

[57] IS 2386 (Part VII), *Methods of test for aggregates for concrete part VII alkali aggregate reactivity*, Bureau of Indian Standards, 1997.

[58] IS 383 1970, *Specification for coarse and fine aggregates from natural sources for concrete*, Bureau of Indian Standards, 1997.

[59] IS 456 2000, "Plain and reinforced concrete-code of practice," Bureau of Indian Standards, 2000.

[60] IS 12119 1987, *General requirement for pan mixtures for concrete*, Bureau of Indian Standards, 1999.

[61] IS: 1199-1959 Reaffirmed, IS 1199 1959, *Methods of sampling and analysis of concrete*, Bureau of Indian Standards, 1959.

[62] IS 9103 1999, *Concrete admixtures-specification*, Bureau of Indian Standards, 1999.

[63] IS 516 1959, *Methods of test for strength of concrete*, Bureau of Indian Standards, 2004.

[64] L. Breiman, "Random forests," *International Journal of Advanced Computer Science and Applications*, vol. 45, pp. 5–31, 2016.